Journal of the Korean Society of Remote Sensing, Vol. 10, No. 2, 1994

A Semi-empirical Model for Microwave Polarimetric Radar Backscattering from Bare Soil Surfaces

Yisok Oh
Department of Radio Science and Engineering
Hong-Ik University, Seoul, Korea

Abstract

A semi-empirical model for microwave polarimetric radar backscattering from bare soil surfaces was developed using polarimetric radar measurements and the knowledge based on the theoretical and numerical solutions. The microwave polarimetric backscatter measurements were conducted for bare soil surfaces under a variety of roughness and moisture conditions at L-, C-, and X-band frequencies at incidence angles ranging from 10° to 70° . Since the accurate target parameters as well as the radar parameters are necessary for radar scattering modeling, a complete and accurate set of ground truth data were also collected using a laser profile meter and dielectric probes for each surface condition, from which accurate measurements were made of the rms height, correlation length, and dielectric constant. At first, the angular and spectral dependencies of the measured radar backscatter for a wide range of roughnesses and moisture conditions are examined. Then, the measured scattering behavior was tested using theoretical and numerical solutions. Based on the experimental observations and the theoretical and numerical solutions, a semi-empirical model was developed for backscattering coefficients in terms of the surface roughness parameters and the relative dielectric constant of the soil surface. The model was found to yield very good agreement with the backscattering measurements of this study as well as with independent measurements.

1. Introduction

The problem of electromagnetic wave scattering from random surfaces have long been studied and because of its complexity theoretical solution exist only for limiting cases. When deviation of the surface profile is slightly different from that of a smooth surface, perturbation solutions can be used. In the classic treatment of small perturbation method (SPM) [Rice, 1951; Tsang et al., 1985] it is required that the rms height be much smaller than the wavelength and the rms slope be same order of magnitude as the wavenumber times the rms height. Recently, a perturbation method based on perturbation expansion of phase of the surface field (PPM) was developed which extends the region of validity of SPM to higher rms height but with modest slope and curvature [Wineberner and Ishimaru, 1985]. The other limiting case is when surface irregularities are large compared to the wavelength, namely the radius of curvature at each point on the surface is large. In this limit the solution is known as Kirchhoff approximation (KA) [Beckmann and Spizzichino, 1963; Ulaby et al., 1982]. Various types of modifications and improvements to this model can be found in literature. In these papers the effects of shadowing and multiple scattering are discussed which basically extends the region of KA slightly [Fung and Eom, 1981]. Combined solution of KA and SPM which is applicable for composite surfaces has basically the same regions of validity as the individual models [Brown, 1978].

At microwave frequencies most of natural surfaces do not fall into the validity regions of the theoretical models. Also a complete set of measured data does not exist to characterize the role of influential parameters in the scattering mechanism. Thus the major goal in this investigation is to find the dependency of the radar backscatter to the roughness parameters and soil moisture condition through extensive backscatter measurement for variety of moisture and roughness conditions and over a wide range of incidence angles and frequencies. Once the dependency of the radar backscatter to these parameters are obtained, the semi-empirical model can be used to retrieve the surface roughness and soil moisture content from measured data.

The radar backscatter of bare soil surfaces under variety of conditions were measured using a truck- mounted network analyzer based scatterometer (The University of Michigan's LCX POLARSCATS) [Tassoudji et al., 1989]. The data were collected polarimetrically at L-, C-, and X-band frequencies at incidence angles ranging from 10° to 70o. A semi-empirical model is formulated based on a set of measured data and another set of data is used to verify the semi-empirical model. Excellent qualitative and reasonable quantitative agreement is obtained.

2. Data Acquisition

The University of Michigan's LCX POLARSCAT [Tassoudji et al., 1989] was designed with the capability to measure the scattering matrix of point or distributed targets at L-, C- and X-band frequencies (1.5, 4.75, and 9.5 GHz of center frequencies, respectively). The scatterometer consists of an automatic vector network analyzer (HP 8753A), a computer unit, a disk drive for data storage, an amplifying and pulsing circuitry for hardware range gating, a relay actuator, and L-, C-, X-band RF circuitries and antennas. Antennas are dual-polarized with orthogonal mode transducers (OMT) to transmit and receive a set of orthogonal polarizations. A computer is used to control the network analyzer through HP-IB (interface bus) to acquire the desired data automatically. The computer also controls a relay actuator which energizes the desired frequency and polarization switches.

To achieve good statistical representation of the measured backscatter for distributed targets, a large number of spatially independent samples are required. In this experiment 90 and 60 independent samples were taken at incidence angles of 10°, 20°, 30°, 40°, 50°, 60°, 70°, respectively. To achieve temporal resolution and also to increase the number of independent samples, measurements were performed over 0.3 GHz for L-band and 0.5 GHz for C- and X-band, assuming backscattering coefficient is constant over the mentioned bandwidths.

In addition to the soil backscatter data, the noise background level was measured by pointing the antennas towards the sky. The noise background level was subtracted from the soil backscatter data coherently to improve the signal to noise ratio. The polarimetric response of a conducting sphere was measured to achieve absolute calibration of the radar system [Sarabandi and Ulaby, 1990, Sarabandi et al., 1992]. To minimize the time elapsed between the four polarization measurements that completes a polarimetric set, the soil backscatter data were collected in a raw-data format. The radar data was post-processed to separate the unwanted short-range returns from the target return using the time domain gating capability. The gated target response was then calibrated using the sphere data.

The height profiles of soil surfaces are measured by the Laser profile meter mounted on a stepper-motor driven XY-table. The Laser profile meter can measure a surface profile with 1 mm horizontal resolution and 2 mm vertical accuracy. A laptop computer is connected to the stepper-motor controllers to position the Laser distance meter with the desired steps in X and Y directions. The heights measured by the Laser distance meter are also collected and stored by the same computer. A minimum of ten one-meter profiles

are collected for each surface with steps of 0.25 cm in the horizontal direction. In addition to the surface profiles acquired by the Laser profile meter, a couple of three-meter-profiles were collected using chart paper and spray paint to monitor large scale roughnesses variations. Radar measurements were conducted for four surface-roughness conditions, covering the range from 0.32 cm to 3.02 cm in rms height.

Dielectric constants of the soil fields were measured by a C-band (4.8 GHz) field-portable dielectric probe [Brunfeldt, 1987]. The probe consists of a reflectometer assembly with a coaxial probe tip and a signal processing assembly with a calculator. Dielectric constants were measured at the top and at the depth of 4 cm for more than fifty spots randomly chosen over each surface. The dielectric constants (εr) were used to estimate the moisture contents (mv) by inverting a semiempirical model [Hallikainen et al., 1985] which gives εr in terms of mv. The real part of εr is chosen since the error in measuring the imaginary part of εr by dielectric probe is relatively high [Jackson, 1990]. The mean value of mv then was used in the same semiempirical model to obtain estimates of εr at L-, C- and X-band frequencies. Soil density was determined from soil samples of which volumes are known.

3. Experimental Data Analysis

In this section we present samples of the measured radar backscatter to demonstrate the spectral, angular, and polarimetric behavior of rough surface backscattering coefficients. Four different fields (S1, S2, S3, and S4) were considered. Each one of four surfaces was measured under two different moisture conditions, relatively wet and relatively dry. The roughness parameters of the surfaces such as rms height s, autocorrelation function $\rho(\xi)$, correlation length l, and rms slope m, are calculated from the measured surface height distributions.

The surface height distributions of all four surfaces fit well to Gaussians distribution. The autocorrelation functions for surfaces 1, 2, and 3, fit better to exponential functions ($\rho(\xi) = \exp[\ -|\xi|/l\ ]$) than to Gaussian functions ($\rho(\xi) = \exp[\ -\xi^2/l^2\ ]$). The Gaussian form provided a better fit for the roughest field, S4. The surface rms slopes can be calculated from $m = s\sqrt{|\rho''(0)|}$, where $\rho''(0)$ is the second derivative of $\rho(\xi)$ evaluated at ξ=0.

Among the four surfaces, surface S2 is the smoothest (s = 0.32 cm), surface S1 (s = 0.4 cm) is slightly rougher, surface S3 (s = 1.12 cm) represents an intermediate-roughness

condition, and surface S4 (s = 3.02 cm) is a very rough surface that was generated by plowing the top 15-cm surface layer. Electromagnetically, these surfaces cover a wide range of roughness conditions, extending from ks = 0.1 to ks = 6.01 (where $k = 2\pi/\lambda$ is the wave number) and from kl = 2.6 to kl = 19.7. Surface 1, for example, may be considered smooth at 1.5 GHz (ks = 0.13, where k is a wave number), and medium rough at 4.75 GHZ and 9.5 GHz (ks = 0.42 and 0.80, respectively). The 12 roughness conditions corresponding to the four surfaces and three wavelengths are identified in ks-kl space in Fig. 3, together with the boundaries for the regions of validity of the small perturbation model (SPM) and the physical optics (PO) and geometrical optics (GO) solutions of the Kirchhoff approximation.

The effect of surface roughness on the angular response of σ° is shown in Fig. 1 which contains plots of the three principal polarization components for the smoothest case (Fig. 1a), corresponding to surface S2 at 1.5 GHz, and for the roughest-surface condition (Fig. 1b), corresponding to surface S4 at 9.5 GHz. Based on these and on the data measured for the other surfaces, we note that the ratio of σ°_{hh} to σ°_{vv}, which will be referred to as the co-polarized ratio, is always smaller than or equal to 1, and it approaches 1 as ks becomes large. Very rough surfaces such as C4 (surface 4 at C-band) and X4 do not show any noticeable differences between σ°_{vv} and σ°_{hh}, while smooth surfaces show values of $\sigma^\circ_{hh}/\sigma^\circ_{vv}$ smaller than 1. It is also observed that co-polarized ratio is a function of incidence angle for smooth surfaces and increases as the incidence angle increases. For very rough surfaces ($ks \geq 2$) $\sigma^\circ_{hh}/\sigma^\circ_{vv} \cong 1$ independent of incidence angle.

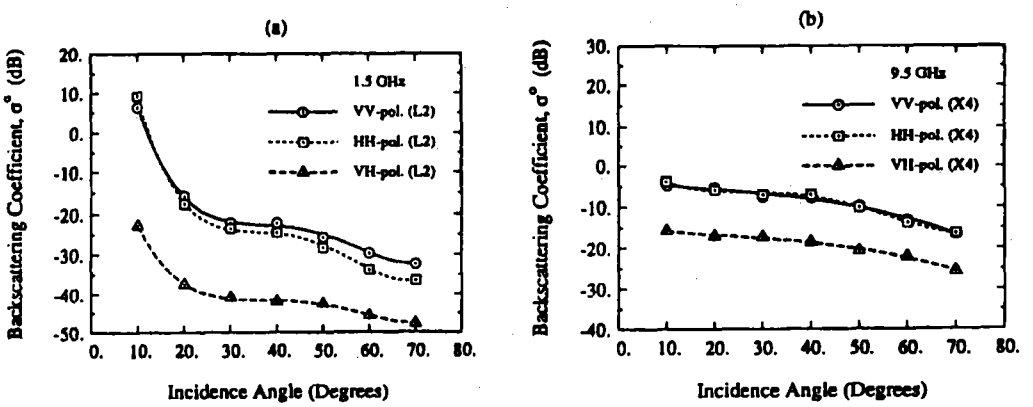

Figure 1. Angular responses of σ°_{vv}, σ°_{hh}, and σ°_{hv} for (a) a smooth surface at 1.5 GHz (L2) and (b) a very rough surface at 9.5 GHz (X4).

Another point worth noting is that the shape of the angular pattern of the cross-polarized backscattering coefficient σ°_{hv}, is similar to that of σ°_{vv}, but the ratio $\sigma^{\circ}_{hv}/\sigma^{\circ}_{vv}$, which will be referred to as cross-polarized ratio, increases with ks as shown in Figs. 1(a), (b) (and more explicitly in Fig. 5).

The backscattering coefficients of a surface is a function of moisture content. Figure 2(a) shows the backscattering coefficient of surface 1 for two moisture conditions, m_v=0.29 and m_v=0.14. The ratio of σ°_{vv} (or σ°_{hv}) of wet soil to σ°_{vv} (or σ°_{hv}) of dry soil is about 3 dB at the angles ranging from 20° to 70°. The sensitivity of σ° to moisture contents (about 3 dB in Fig. 2(a)) is much lower than the sensitivity to surface roughness (about 16 dB between smooth and very rough surfaces) in this experiment. Figure 2(b) shows the angular response of the co-polarized ratio $\sigma^{\circ}_{hh}/\sigma^{\circ}_{vv}$ for a fixed roughness at two different moisture contents. The magnitude of the co-polarized ratio is larger for the wet surface (6 dB at 50°) than for the dry surface (3 dB at 50°).

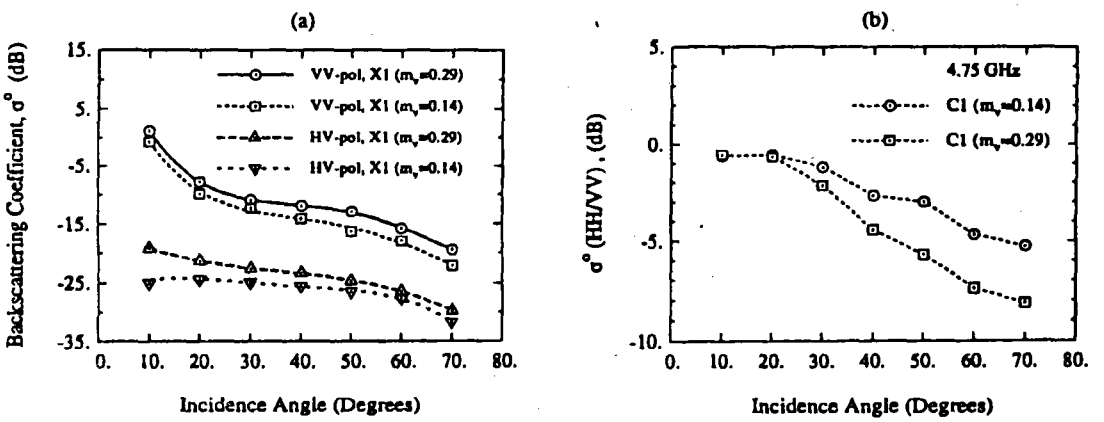

Figure 2. Angular plots of (a) σ°_{vv} and σ°_{hv} of surface S1 at X-band for two different moisture conditions and (b) the like-polarized ratio, σ°_{hh} / σ°_{vv}, for the same surface at C-band.

4. Theoretical and Numerical Solutions

This section evaluates the applicability of the small perturbation method (SPM), the physical optics (PO) model, and the geometrical optics (GO) model to the measured radar data. Next, a numerical solution for backscattering from one-dimensional conducting

surfaces has been studied to examine the general trends of backscattering coefficients.

The theoretical solutions for rough surface backscattering are compared with experimental data where applicable. Expressions for the backscattering coefficient and the region of validity of these models are given in [Oh, 1993, Ch. 2]. Measured roughnesses for all four surfaces at three frequencies are shown in Fig. 3 in terms of ks and kl. Also shown are the regions of validity of the models; SPM, PO, GO models.

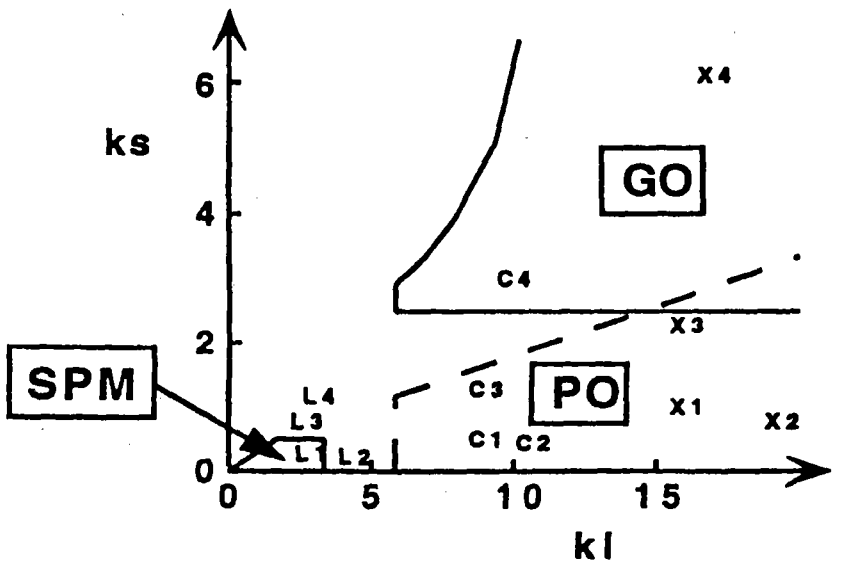

Figure 3. Roughness parameters and the region of validity of SPM, PO, and GO models.

The lower limit of the ks value of the validity region for GO model given by $ks > \sqrt{2.5}/\cos\theta$ is chosen at the incidence angle θ of 30°, where the lower limit varies from ks = 1.62 at θ=10° to ks = 6.32 at θ = 60°.

4.1 Small Perturbation Model

The small perturbation model (SPM) is applicable only on L1 (surface 1 at L-band frequencies) according to Fig. 3. The backscattering coefficients computed by SPM for an exponential autocorrelation function are compared with those measured for L1, and the results show that the backscattering coefficients of SPM with exponential autocorrelation function fits better to the measured ones than those with a Gaussian autocorrelation

function, even though there is about 5 dB discrepancies at higher incidence angles. The measured σ°_{hh} agrees quite well with SPM model (within about 1 dB tolerance) when exponential autocorrelation is assumed. As mentioned earlier, the measured autocorrelation function of surface 1 fits better to exponential than to Gaussian autocorrelation function. The cross-polarized backscattering coefficient for L1 computed using the second-order SPM with exponential autocorrelation function shows that the angular trend of the calculated σ°_{hv} fits well to that of the measured σ°_{hv} while the values of the measured σ°_{hv} are higher than those of the SPM. The similar discrepancy between another theoretical model (Integral Equation Methd) and the measurements for the cross-polarized backscattering coefficient is also reported in [Fung et al., 1992].

4.2 Physical Optics Model

Several roughnesses of this experiment, C1, C2, C3, X1, X2, and X3, are in the region of validity of the physical optics (PO) Model. One case of those roughnesses, X1, is closely examined and the results show that the *vv*-polarized backscattering coefficient σ°_{vv} modeled by PO with Gaussian autocorrelation function deviates from the measured σ°_{vv} except at small incidence angles, but σ°_{vv} modeled by PO with exponential autocorrelation function agrees to the measured σ°_{vv} quite well over a wide range of angles $\theta<40^{\circ}$. The comparison between σ°_{hh} of PO model and σ°_{hh} measured for the surface of X1 shows similar result.

The *hh*-polarized backscattering coefficients σ°_{hh} of the PO model agree, within about 3 dB, to the measured values for the surfaces of C2, C3, and X1 at the angles less than 40°. The *vv*-polarized backscattering coefficients σ°_{vv} of the PO model, however, deviate much from the measured values for all surfaces. The deviation is very large at large incidence angles ($\theta \geq 50^{\circ}$).

PO model failed on the prediction of σ° for the most surfaces which roughness parameters are in the region of validity of the PO model. The cross polarization backscattering coefficient is not available for PO model. The measured σ°_{vv} is higher than or equal to σohh in all cases of roughnesses, moisture contents, and incidence angles, which is contrary to the PO model. This is due to the fact that σ°_{vv} and σ°_{hh} of the PO model are directly proportional to the Fresnel reflectivities.

4.3 Geometrical Optics Model

The geometrical optics (GO) model agrees with the measured σ°_{vv} and σ°_{hh} within 4 dB

tolerance for C4 case and within about 2 dB tolerance for X4 for the incidence angles less than or equal to 50°. The coherent component of the backscattering coefficient is negligibly small for the very rough surfaces like C4 and X4, and the noncoherent component dominates at all angles including normal incidence. The GO model like the PO model is incapable of predicting the cross-polarized terms. This model also failed to predict σ^o_{vv} (or σ^o_{hh}) at larger incidence angle ($\theta > 60°$).

The major conclusions we drew from our analysis of the measured radar data when compared with the predictions of the SPM, PO, and GO models are: (1) Some natural surface conditions fall outside the regions of validity of all three models. (2) None of the models provides consistently good agreement with the measured data, particularly at incidence angles greater than 40°. (3) The PO model predicts that $\sigma^o_{vv} < \sigma^o_{hh}$, contrary to all observations. Additionally, being first-order solutions, both the PO and GO models cannot be used for σ^o_{hv}. Faced with these inadequacies of the available theoretical scattering models, we decided to develop a semi-empirical model that relates σ^o_{vv}, σ^o_{hh}, and σ^o_{hv} to the roughness (ks) and dielectric constant ε_r of the surface.

4.4 Method of Moments Solution

In order to examine the general angular and spectral trends of the backscattering coefficients, a numerical simulation method for backscattering from one-dimensional conducting surfaces is obtained to predict exact backscattering coefficients [Oh and Sarabandi, 1994]. At first, a standard method for a random surface generation will be introduced in case of the surface with a Gaussian correlation function. Then, a formulation of the method of moments will be reviewed briefly for vv- and hh-polarized backscattering coefficients.

4.4.1 Random Surface Generation

A sequence of independent Gaussian deviates with zero mean and unit variance (N[0,1]) can be obtained from a standard routine [Press et al., 1986]. Then these independent Gaussian deviates can be correlated to a specific correlation function using the concept of digital filtering [Fung and Chen, 1985]. The desired surface height profile $\{Z(k)\}$ can be written as the summation of the product of the independent Gaussian deviates $\{X(j+k)\}$ and a discrete weighting factor $\{W(j)\}$ which is to be determined,

$$Z(k) = \sum_{j=-M}^{M} W(j)\ X(j+k), \tag{1}$$

where $Z(k)$ is the kth point of a discrete height profile and M is the total number of sample points of the weighting factor $W(j)$. When a correlation coefficient function $C(i)$ of the desired surface profile is given as a Gaussian function as follows;

$$C(i) = s^2 \exp\left[-\left(\frac{i}{L}\right)^2 \right], \tag{2}$$

the corresponding weight factor can be obtained as

$$W(j) = s\sqrt{\frac{2}{\sqrt{\pi L}}}\ \exp\left[-2\left(\frac{j}{L}\right)^2 \right], \tag{3}$$

where s is the standard deviation of the height distribution (rms height), L is the discrete number given as $l/\Delta x$, l is the correlation length of a random surface, and Δx is the sampling interval. Then, the surface height profile can be computed by (1)-(3) for given surface statistics such as the rms height, the correlation function. The proper value for the width of an independent surface D and the sampling interval Δx is a function of the surface correlation length and frequency of the incident wave.

4.4.2 Formulation of the Method of Moments

The scattered field can be represented by the convolution of the surface current density $\overline{J_e}$ and the Green's function as follows:

$$\overline{E^s}(\overline{\rho}) = -\frac{k_o Z_o}{4} \int_l \overline{J_c}\,(\overline{\rho})\ H_o^{(1)}(k_o|\overline{\rho}-\overline{\rho'}|)\ dl', \tag{4}$$

where k_o and Z_o are the wave number and the intrinsic impedance of free space, respectively. $H_o^{(1)}$ is the zeroth order Hankel function of the first kind, and $\overline{\rho}$ and $\overline{\rho'}$ are the position vectors of observation and source points, respectively. The surface current density $\overline{J_e}(\overline{\rho'})$ due to the incident plane wave is to be determined numerically by the method of moments (MoM) [Harrington, 1968].

For the solution of *hh*-polarization case, the electric field integral equation (EFIE) for one-dimensional conducting surface can be written as

$$\overline{E^i}(\overline{\rho}) = \frac{k_o Z_o}{4} \int_l \overline{J_c}\,(\overline{\rho'})\ H_o^{(1)}(k_o|\overline{\rho}-\overline{\rho'}|)\ dl', \quad \overline{\rho'} \text{ on interface} \tag{5}$$

The simplest MoM solution of (5) consists of using the pulse basis and point matching. After discretizing a sample surface into M (=D/Δx) cells, the pulse basis function can be applied. Then, (5) can be casted into a matrix equation using the point matching technique,

$$[\ Z_{mn}]\ \ [\ I_n]\ \ =\ \ [\ V_m] \tag{6}$$

where $[I_n]$ is the surface current vector which is to be determined.

Once the surface current vector $[I_n]$ is found, the hh-polarized scattered field, Eshh, in the far-field can be computed using the far-field approximation of $H_o^{(1)}(k_o\,\rho)$.

$$E_{hh}^{s}(\theta_s) = -\frac{k_o Z_o}{\sqrt{8\pi k_o \rho}} \exp[\ i(k_o\rho - \pi/4)]\ \ \sum_{n=1}^{M} I_y(x_n, z_n)\ \exp[\ -ik_o\hat{k_s}\cdot\overline{\rho_n}]\ \ \triangle x_n \sqrt{1+\left(\frac{dz_n}{dx_n}\right)} \tag{7}$$

For the solution of vv-polarization case, the magnetic field integral equation (HFIE) can be used to compute the surface current as follows:

$$-\hat{n}\times\overline{H^{i}}(\overline{\rho}) = -\frac{1}{2}\overline{J_c}(\overline{\rho}) + \frac{i}{4}\int_l \hat{n}\times\{\overline{J_c}(\overline{\rho'})]\ \times\nabla H_o^{(1)}(k_o|\overline{\rho}-\overline{\rho'}|)\}\ dl', \quad \overline{\rho'} \text{ on interface} \tag{8}$$

The vv-polarized scattered field in the far-field can be computed similarly as

$$\begin{aligned} E_{vv}^{s}(\theta_s) \ = \ -\frac{k_o Z_o}{\sqrt{8\pi k_o \rho}} \exp[\ i(k_o\rho - \pi/4)]\ \ \sum_{n=1}^{M}\left[\ -\cos\theta_s + \sin\theta_s \frac{dz_n}{dx_n}\right]\ I_y(x_n, z_n) \\ \cdot\ \exp[\ -ik_o\hat{k_s}\cdot\overline{\rho_n}]\ \ \triangle x_n \sqrt{1+\left(\frac{dz_n}{dx_n}\right)}. \end{aligned} \tag{9}$$

In order to suppress the effect of the edges of a finite surface sample, which results from the limitation of computer storage and speed, a properly tapered resistive sheet can be added at the end of each finite surface. An exact numerical solution can be obtained using this resistive sheet technique even at large incidence angles [Oh and Sarabandi, 1994].

5. A Semi-Empirical Model

The failure of existing models to cover roughness conditions that occur more often in nature as described in the previous section, prompts development of semi-empirical backscattering models for random surfaces. Another reason for developing the semi-empirical model is to generate an inversion algorithm to retrieve soil moisture and surface roughness from the measured radar backscatter.

Semi-empirical models of backscattering coefficients, σ°_{vv}, σ°_{hh} and σohv are developed based on the measured radar backscatter and knowledge of theoretical and numerical scattering solutions. For this set of data, surface roughnesses and the volumetric moisture contents are in the range of $0.1<ks<6.0$, $2.6<kl<19.7$, and $0.09<mv<0.31$, which is the region of interest at microwave frequencies.

5.1 Development

We begin with an examination of the cross-polarized ratio $q=\sigma^{\circ}_{hv}/\sigma^{\circ}_{vv}$. The angular pattern of σ°_{hv} follows the pattern of σ°_{vv} and the cross-polarized ratio is a function of roughness and frequency as shown previously. Cross-polarized ratio increases when frequency and/or surface rms height s increases.

The angular trend and the dependency of the cross-polarized ratio on the rms height, the correlation length, and the dielectric constant are examined using the SPM as shown in Figs. 4 (a), (b), and (c), respectively. According to the SPM, the cross-polarized ratio increases rapidly as the value of ks increases, and shows very weak dependency on the value of kl and the dielectric constant. These trends are very similar to the measurements.

Figs. 5 (a) and (b) show the variation of the measured cross-polarized ratio $\sigma^{\circ}_{hv}/\sigma^{\circ}_{vv}$ as a function of ks which includes both frequency and rms height, for incidence angles of 30°, 40° and 50°. The cross-polarized ratio starts from values of about -20 dB for $ks\cong 0.1$ and increases linearly with ks until $\sigma^{\circ}_{hv}/\sigma^{\circ}_{vv}$ saturates at values about -10 dB ($ks\geq 2$) as shown in Fig. 5(a). Cross-polarized ratios for the relatively wet surfaces start from smaller values than those for the relatively dry surfaces and increases more rapidly as ks increases, and the ratio saturates at higher values (about -9 dB) as shown in Fig. 5(b). A semi-empirical form for the cross-polarized ratio $\sigma^{\circ}_{hv}/\sigma^{\circ}_{vv}$ is obtained by curve fitting of the measured data as follows:

$$q \equiv \frac{\sigma^{o}_{hv}}{\sigma^{o}_{vv}} = 0.25\sqrt{\Gamma_o}\,[\,0.1+(\sin\theta)^{0.9}]\,\{1-\exp[\,-(1.4-1.6\Gamma_o)ks]\,\} \quad (10)$$

where Γo is the Fresnel reflectivity of the surface at nadir, $\Gamma_o = \left|\frac{1-\sqrt{\varepsilon_r}}{1+\sqrt{\varepsilon_r}}\right|^2$.

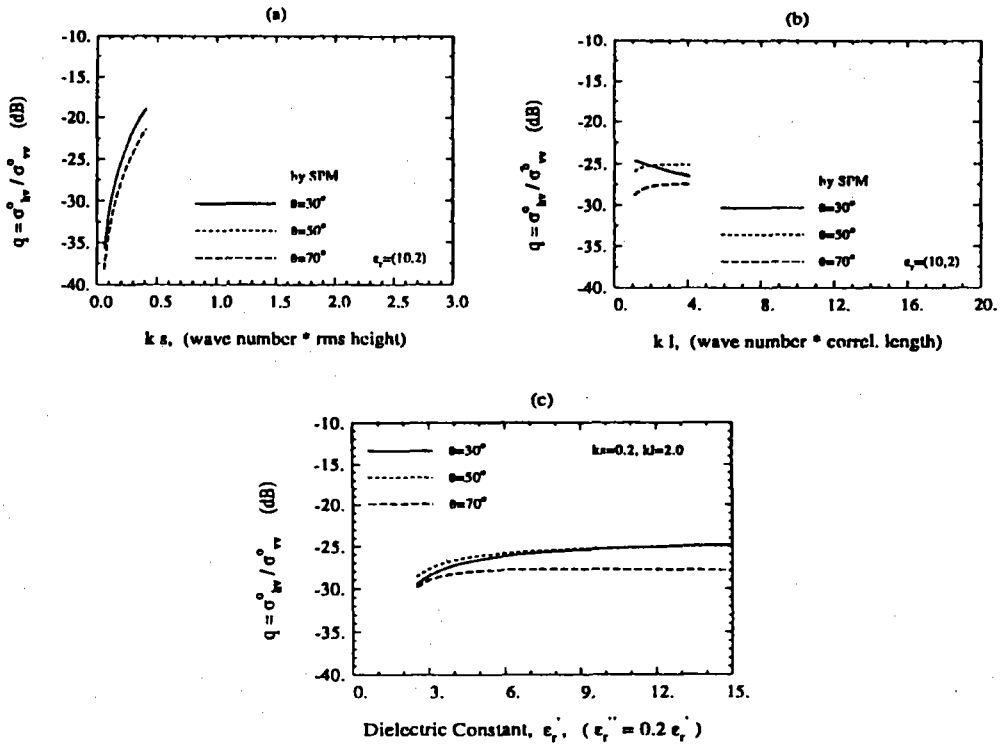

Figure 4. The SPM solutions of the cross-polarized ratio $q=\sigma^{\circ}_{hv}/\sigma^{\circ}_{vv}$ to examine the dependency on (a) *ks*, (b) *kl*, and (c) the dielectric constant

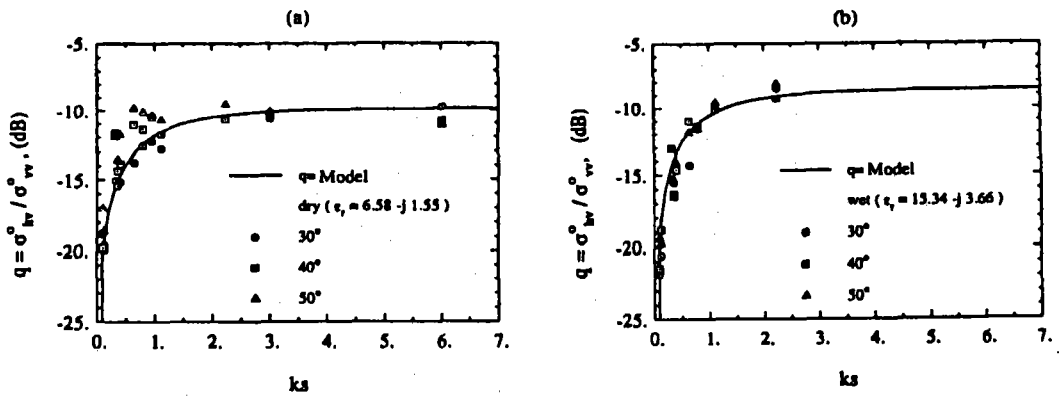

Figure 5. The sensitivity of the cross-polarized ratio, $\sigma^{\circ}_{hv}/\sigma^{\circ}_{vv}$ to surface roughness for (a) dry soil and (b) wet soil surfaces.

Figures 5(a) and (b) also shows the semi-empirical function for the cross-polarized ratio compared with the measured data.

Next, the co-polarized ratio $p=\sigma^{\circ}_{hh}/\sigma^{\circ}_{vv}$ is examined. The measured values of the co-polarized ratio is a function of surface roughness, soil moisture content, and incidence angle. In order to verify the dependency of the co-polarized ratio on surface roughness and dielectric constant, the theoretical and the Method of Moment solutions are examined as shown in Figs. 6 (a) and (b). Figure 6 (a) shows the dependency of the ratio on ks for dielectric surfaces (by SPM and GO models) and conducting surfaces (by the Method of Moments solution). Figure 6 (b) shows the effect of soil moisture on the co-polarized ratio, and these trends agree with the measured co-polarized ratios.

Figures 7(a) and (b) show the variation of the measured ratio $\sigma^{\circ}_{hh}/\sigma^{\circ}_{vv}$ with respect to the roughness parameter ks for both of wet and dry conditions at the incidence angles of 40° and 50°, respectively. The co-polarized ratios start from -7.5 dB for wet soil and -4.5 dB for dry soil at 50° incidence, which are much lower than those for 40° incidence. Both of Fig. 7(a) and (b) show that the co-polarized ratio $\sigma^{\circ}_{hh}/\sigma^{\circ}_{vv}$ of wet soil are lower than those of the dry soil. The curves shown in Fig. 7 are based on the empirical expression

$$\sqrt{p} = 1-\left(\frac{2\theta}{\pi}\right)^{0.314/\Gamma_o} \cdot \exp[\,-ks] \ . \tag{11}$$

where θ is the incidence angle in radians.

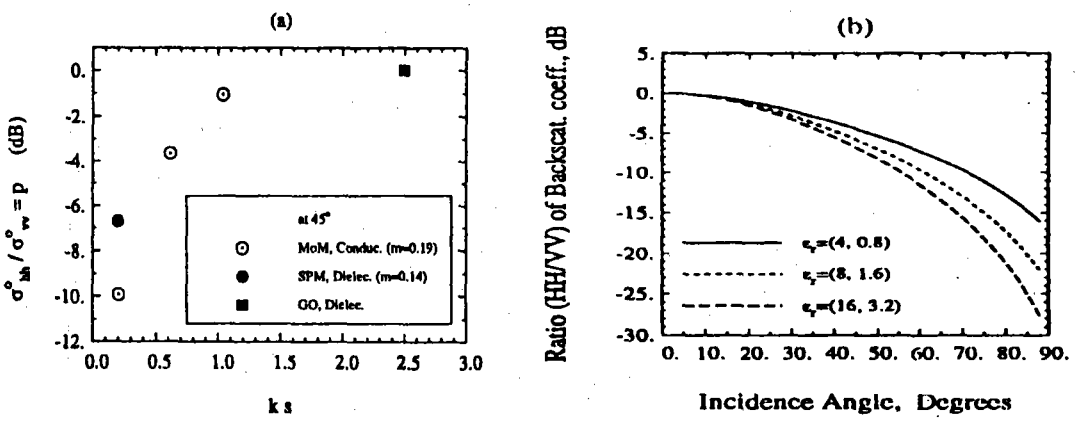

Figure 6. Examination of the co-polarized ratio $p=\sigma^{\circ}_{hh}/\sigma^{\circ}_{vv}$; (a) dependency on ks using the SPM, the GO, and the Method of Moments, and (b) the angular response for different dielectric constants using the SPM.

Having established semi-empirical formulas for $q=\sigma^{\circ}_{hv}/\sigma^{\circ}_{vv}$ and $p=\sigma ohh\ /\sigma^{\circ}_{vv}$ that provide reasonable agreement with the measured data, the remaining task is to relate the absolute level of any one of the three linearly polarized backscattering coefficients to the surface parameters. At first, the measured correlation function was modeled by a quadratic-exponential function given by

$$\rho(\xi) = \left\{1-\frac{\xi^2}{(al)^2}\right\}\cdot \exp\left[-\frac{\xi}{bl}\right] \tag{12}$$

where a and b are constants and l is the correlation length.

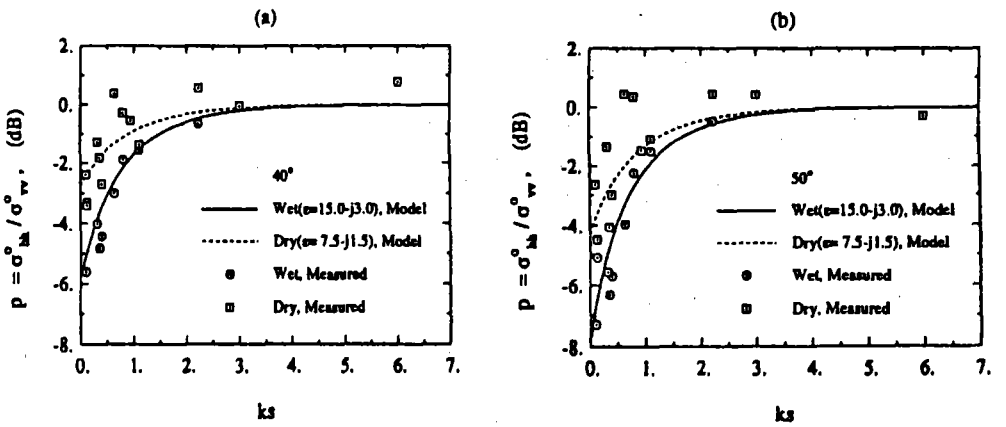

Figure 7. The sensitivity of the co-polarized ratio, $\sigma^{\circ}_{hh}/\sigma^{\circ}_{vv}$, to surface roughness and soil moisture at (a) 40° and (b) 50°.

Based on the theoretical models, a functional form of the vv-polarized backscattering coefficients were chosen, and the unknown constants of the expression were obtained using the measured data. Upon comparison the expression with the measured data, an semi-empirical formula for the backscattering coefficient σ°_{vv} is found to have the following form:

$$\sigma^{\circ}_{vv} = 13.5\ \exp\left[-1.4(ks)^{0.2}\right]\frac{1}{\sqrt{p}}\Gamma_h\,(ks)^2\,(\cos\theta)^{3.25-0.05kl}\cdot \exp\left[-(2ks\cos\theta)^{0.6}\right]\ W_k \tag{13}$$

where Wk is the roughness spectrum corresponding to the quadratic-exponential correlation function, which is given by

$$W_k = \frac{(kl)^2}{1+(2.6\ kl\ \sin\theta)^2}\left[1-0.71\frac{1-3(2.6\ kl\ \sin\theta)^2}{1+(2.6\ kl\ \sin\theta)^2]^{\ 2}}\right] \tag{14}$$

and

$$\Gamma_h = \left| \frac{\cos\theta - \sqrt{\varepsilon_r - \sin^2\theta}}{\cos\theta + \sqrt{\varepsilon_r - \sin^2\theta}} \right|^2 \tag{15}$$

Consequently, the backscattering coefficient σohh and σohv (= σovh) can be obtained as:

$$\sigma^o_{hh} = p\,\sigma^o_{vv}\,, \qquad \sigma^o_{hv} = q\,\sigma^o_{vv} \tag{16}$$

As we will see next, the semi-empirical model was found to provide a good representation of the measured data at all frequencies and over a wide angular range. The model was evaluated against two data sets: (a) the data measured in this study, (b) another independently measured data set that was not used in the development of this model, which shall be referred to as Independent Data Set.

5.2 Comparison With Measured Data

Because of the space limitations, we will present only one typical example illustrating the behavior of the semi-empirical model, in comparison with the data measured in this study. This is shown in Fig. 8 for surface S1 (representing a very smooth surface with s = 0.40). Very good agreement is observed between the model and the measured data at all three frequencies and across the entire angular range between 20° and 70°. After the measurements reported in this study, another data set was acquired by the same radar system with different antenna systems at different frequencies for four surface roughnesses. An evaluation of the semi-empirical model was conducted by comparing its prediction with the backscatter data of Independent Data Set and found the agreement to be very good as shown in Figs. 9 (a) and (b).

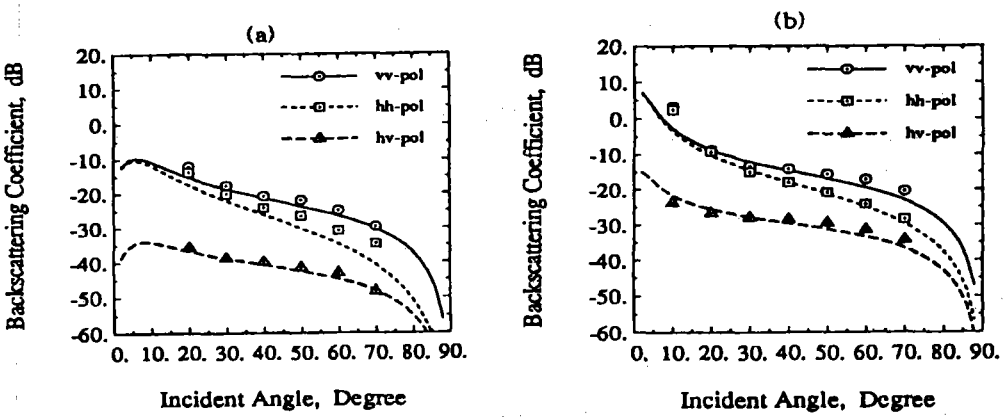

Figure 8. Empirical model compared to the measured data of surface 1 for wet soil at (a) 1.5 GHz and (b) 4.75 GHz.

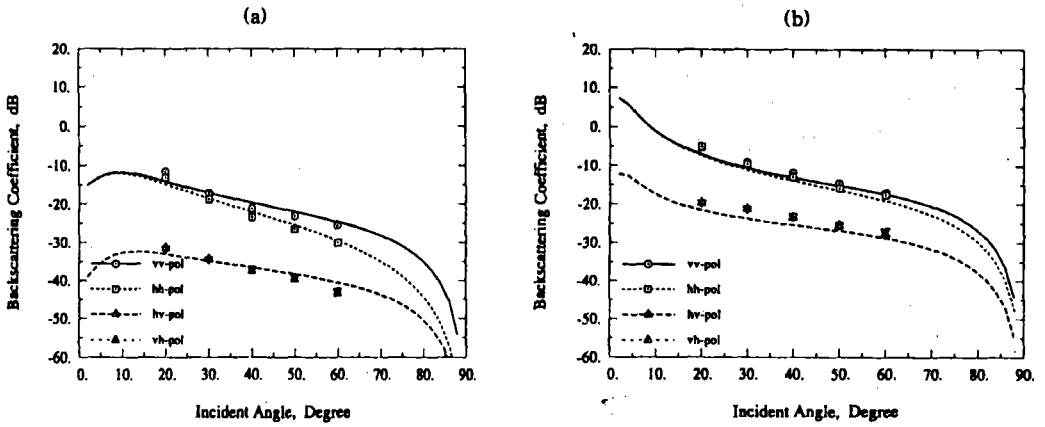

Figure 9. Empirical model compared with the data from Independent Data Set for a surface with s = 0.94 cm and l = 6.24 cm, measured at (a) 1.25 GHz and (b) 5.3 GHz.

6. Conclusions

The major results of this study are summarized as follows: (1) At microwave frequencies, the available rough-surface scattering models are incapable of predicting the scattering behavior observed for bare-soil surface. (2) The co-polarized ratio $p = \sigma^{\circ}_{hh}/\sigma^{\circ}_{vv} \leq 1$ for all angles, roughness conditions, and moisture contents; for all values of incidence angle, roughness, and moisture contents. The ratio p increases rapidly with increasing ks up to $ks \cong 1$, then it increases at a slower rate, reaching the value 1 for $ks > 3$. For $ks < 3$, p decreases with increasing incidence angle and with increasing moisture content. (3) The cross-polarized ratio $q = \sigma^{\circ}_{hv}/\sigma^{\circ}_{vv}$ exhibits a strong dependence on ks and a relatively weak dependence on moisture content. The ratio q increases rapidly with increasing ks up to $ks \cong 1$, then it increases at a slower rate, reaching the value (that depends on the moisture content) for $ks > 3$. (4) The proposed scattering model (SEM) provides very good agreement with experimental observations made over the ranges $0.1 \leq ks \leq 6.0$, $2.5 \leq kl \leq 20.0$, and $0.09 \leq mv \leq 0.31$. The model was found to be equally applicable when tested against radar data independently measured for different surfaces at different frequencies.

Acknowledgments

The author wishes to acknowledge Professors K. Sarabandi and F.T. Ulaby of the Radiation Laboratory in the University of Michigan for their brilliant advices. This work was supported in part by NASA/USA while the author was in the University of Michigan, and is being supported by KSEF under grant 951-916-125-2 for the continuation of this research.

References

Beckmann, P. and A. Spizzichino, 1987, *The Scattering of Electromagnetic Waves from Rough Surfaces*, Artech House.

Brown, G.S., 1978, "Backscattering from a Gaussian Distributed Perfectly Conducting Rough Surface", *IEEE Trans. Antennas Propagat.*, vol. AP-26, pp. 472-482.

Brunfeldt, D.R., 1987, "Theory and Design of a Field-Portable Dielectric Measurement System", *IEEE International Geoscience and Remote Sensing Symposium (IGARSS) Digest* vol. 2, pp. 907-909.

Fung, A.K. and H.J. Eom, 1981, "Multiple Scattering and Depolarization by a Randomly Rough Kirchhoff Surfaces", *IEEE Trans. Antennas Propagat.*, vol. AP-29, pp. 463-471.

Fung, A.K. and M.F. Chen, 1985, "Numerical Simulation of Scattering from Simple and Composite Random Surfaces", *J. Opt. Soc. Am. A*, vol. 2, No. 12, pp. 2274-2284.

Fung, A.K., Z. Li, and K.S. Chen, 1992, "Backscattering from a Randomly Rough Dielectric Surface", *IEEE Trans. Geosci. Remote Sensing*, vol. 30, pp. 356-369.

Hallikainen, M.T., F.T. Ulaby, M.C. Dobson, M.A. El-Rayes, and L. Wu, 1985, "Microwave Dielectric Behavior of Wet Soil -Part-I: Empirical Models and Experimental Observations", *IEEE Trans. Geosci. Remote Sensing*, vol. 23, pp. 25-34.

Harrington, R.F., 1961, *Time-Harmonic Electromagnetic Fields*, McGraw-Hill, New York.

Harrington, R.F., 1968, *Field Computation by Moment Methods*, Macmillan, New York.

Jackson, T.J., 1990, "Laboratory Evaluation of a Field-Portable Dielectric/Soil-Moisture Probe", *IEEE Trans. Geosci. Remote Sensing*, vol. 28, pp. 241-245.

Oh, Y., K. Sarabandi, and F.T. Ulaby, 1992, "An Emperical Model and an Inversion Technique for Radar Scattering from Bare Soil Surfaces", *IEEE Trans. Geosci. Remote Sensing*, vol.30, no.2, pp.370-381, March 1992.

Oh, Y., 1993, *Microwave Polarimetric Backscattering from Natural Rough Surfaces*, Ph.D. Thesis, The University of Michigan, Ann Arbor.

Oh, Y. and K. Sarabandi, 1994, "An Improved Numerical Simulation of Electromagnetic Scattering from Perfectly Conducting Random Surfaces", *IEEE Trans. Geosci. Remote Sensing*, Submitted for publification.

Press, W.H., B.P. Flannery, S.A. Teukolsky, and W.T. Vetterling, 1986, *Numerical Recipes: The Art of Scientific Computing*, University Press, Cambridge, Massachusetts.

Rice, S.O., 1951, "Reflection of Electromagnetic Waves by Slightly Rough Surfaces", *Communication in Pure and Applied Mathematics*, vol. 4, pp. 351-378.

Sarabandi, K., F.T. Ulaby, and M.A. Tassoudji, 1990, "Calibration of Polarimetric Radar Systems with Good Polarization Isolation", *IEEE Trans. Geosci. Remote Sensing*, vol. 28, No. 1, pp. 70-75.

Sarabandi, K. and F.T. Ulaby, 1990, "A Convenient Technique for Polarimetric Calibration of Radar Systems", *IEEE Trans. Geosci. Remote Sensing*, vol. 28, pp. 1022-1033.

Sarabandi, K., Y. Oh, and F.T. Ulaby, 1992, "Measurement and Calibration of Differential Mueller Matrix of Distributed Targets", *IEEE Trans. Antennas Propagat.*, vol. 40, pp. 1524-1532.

Tassoudji, M.A., K. Sarabandi, and F.T. Ulaby, 1989, "Design Consideration and Implementation of the LCX Polarimetric Scatterometer (POLARSCAT)", *Radiation Laboratory Report* No. 022486-T-2, The University of Michigan.

Tsang, L., J.A. Kong, and R.T. Shin, 1985, *Theory of Microwave Remote Sensing*, John Wiley and Sons, New York.

Ulaby, F.T., M.K. Moore, and A.K. Fung, 1982, *Microwave Remote Sensing*, Active and Passive, vol. 2, Artech House, Norwood, MA, U.S.A.

Ulaby, F.T. and C. Elachi, 1990, *Radar Polarimetry for Geoscience Applications*, Artech House, Norwood, MA, U.S.A.

Wineberner, D. and A. Ishimaru, 1985, "Investigation of a Surface Field Phase Perturbation Technique for Scattering from Rough Surfaces", *Radio Sci.*, vol. 20, pp. 161-170.